water

MDPI

*Article*

# Spatial–Temporal Changes in Shallow Groundwater Quality with Human Health Risk Assessment in the Luxi Plain (China)

**Na Yu [1,2,3], Yufeng Lv [2,*], Guang Liu [4,*], Fulei Zhuang [4] and Qian Wang [1,3]**

[1] School of Geography and Environment, Liaocheng University, Liaocheng 252000, China; yuna1@lcu.edu.cn (N.Y.); qianwang@lcu.edu.cn (Q.W.)
[2] Department of Irrigation and Drainage, China Institute of Water Resources and Hydropower Research, Beijing 100038, China
[3] Institute of Huanghe Studies, Liaocheng University, Liaocheng 252000, China
[4] Liaocheng Hydrology Center, Liaocheng 252000, China; lczfl68@163.com
* Correspondence: lvyf@iwhr.com (Y.L.); crazymid@163.com (G.L.); Tel.: +86-186-1081-7665 (Y.L.); +86-135-0635-9672 (G.L.)

**Abstract:** Groundwater is an essential water source for drinking, domestic, irrigation and industrial production in Luxi Plain, Shandong Province, China. Understanding the spatial–temporal changes in groundwater quality and its influencing factors in the region were required for better utilization of groundwater resources and efficient design of groundwater management strategies. In this study, the hydrochemical characteristics of groundwater in the study area were analyzed, and significant evolution was found from 2018 to 2020 due to silicate and carbonate weathering, evaporation and human activities. Moreover, the entropy water quality index (EWQI) was used to assess groundwater quality from 2018 to 2020. The EWQI values in 2018–2020 were 129.5, 90.5 and 94.0, respectively, and 31.7% of the groundwater in 2019 and 20.0% in 2020 can be used directly for drinking in the study area; others can be used for domestic water or irrigation. The potable groundwater, with an EWQI value of <50 (ranked as class I or II water quality), was mainly distributed in the west and southeast of the study area. The potential health risk due to oral intake and dermal intake was further assessed based on the human health risk assessment (HHRA) model. The results showed that, 37.3%, 6.7% and 3.3% of the groundwater samples for adults exceeded the acceptable limit for non-carcinogenic risk of 1.0 in 2018–2020, while for children, they were 88.2%, 30.0% and 56.7%, respectively. The high non-carcinogenic risks virtually all occurred in the counties or districts with higher agricultural or economic values. This work may provide useful information for local groundwater conservation and management and help to ensure a sustainable and healthy water supply for drinking, domestic and agricultural needs.

**Keywords:** spatial–temporal changes; groundwater quality; human health risk assessment; Luxi Plain



**Citation:** Yu, N.; Lv, Y.; Liu, G.; Zhuang, F.; Wang, Q. Spatial–Temporal Changes in Shallow Groundwater Quality with Human Health Risk Assessment in the Luxi Plain (China). *Water* **2023**, *15*, 4120. https://doi.org/10.3390/w15234120

Academic Editor: Dimitrios E. Alexakis

Received: 19 October 2023
Revised: 18 November 2023
Accepted: 25 November 2023
Published: 28 November 2023



## 1. Introduction

Groundwater is one of the world's most important natural water resources for drinking, domestic, irrigation and industrial purposes [1]. However, global climate change and excessive human activities have put severe stress on groundwater resources [2]. Groundwater quality deterioration is one of the leading problems, especially in arid and semi-arid regions where surface water and precipitation are scarce and unevenly distributed [3,4]. More efforts have been made for groundwater quality monitoring, which allows for the comparison of water quality parameters with drinking water standards to determine its suitability for drinking purposes [5]. However, in order to better understand the causes of changes in groundwater quality and to determine its appropriate use, it is necessary to conduct a comprehensive assessment of groundwater quality. Moreover, a health risk assessment is required for supporting groundwater quality assessment and environmental management.

To date, various methods have been applied to assess the water quality, including a set pair analysis model (SPA), multivariate statistical technique and entropy-weighted technique [6–8]. Among these methods, the entropy-weighted water quality index (EWQI) can reduce the large amounts of data into a single and informative value by assigning different entropy weights to each parameter according to its relative importance in the overall water quality [9,10]. It is accurate and reliable for reflecting the overall groundwater quality and has been widely used around the world [11,12]. However, most studies based on EWQI have focused on spatial scales or relatively short temporal scales, such as dry and wet seasons within a year [8,13,14]. Previous studies showed that there were no significant changes in groundwater chemistry within a year [8,13]. Therefore, it is necessary to identify the interannual variability in groundwater quality in a specific region.

Luxi Plain, located in the west of Shandong Province, is a typical semi-arid plain. It is a major grain-producing area that plays a significant role in the national grain supply. Groundwater is the main water source for drinking and irrigation in this surface water-scarce region. For example, as the hinterland of Luxi Plain, the local surface water supply of Liaocheng was only $1.4 \times 10^9$ $m^3$ in 2021, while the groundwater supply was $6.4 \times 10^9$ $m^3$, accounting for 39.4% of the total water supply [15]. However, compared to other regions in the world (Table S1), groundwater quality in some areas has been seriously affected by human activities, making the groundwater unsuitable for drinking. For example, it has been reported that the quality of shallow groundwater in the suburbs of Liaocheng is poor, with agricultural fertilization being the main pollution source [16]. At present, few studies have conducted a comprehensive groundwater quality assessment in this region. In light of this, the specific objectives were (i) to analyze the interannual variability in groundwater hydrochemical characteristics and identify their controlling factors in recent years, (ii) to determine groundwater quality and its appropriate use based on the method of EWQI and (iii) to assess the potential health risks associated with exposure to the representative toxicological substances (manganese, nitrate, nitrite and fluoride) in the groundwater of this region. These outcomes are expected to provide a scientific basis for a comprehensive understanding of the groundwater quality and for finding suitable drinking water sources in the study area.

## 2. Materials and Methods

### *2.1. Study Area*

#### 2.1.1. Location and Climate

The study area was Liaocheng City, Shandong Province, which is known as the hinterland of Luxi Plain. It covers approximately 8715 $km^2$ and is located between 116°16′ E to 116°32′ E and 35°47′ N to 37°05′. The prefecture-level city of Liaocheng administers eight county-level divisions, including two districts (Dongchangfu, Chiping), one county-level city (Linqing) and five counties (Donge, Gaotang, Guangxian, Shenxian and Yanggu) (Figure 1). Liaocheng features a semi-arid continental climate, with low precipitation and intensive evaporation. The average annual precipitation and evaporation in this area are 578.7 mm and 1708.7 mm, respectively. Half of the precipitation is concentrated from June to August, while the minimum rainfall is in January.

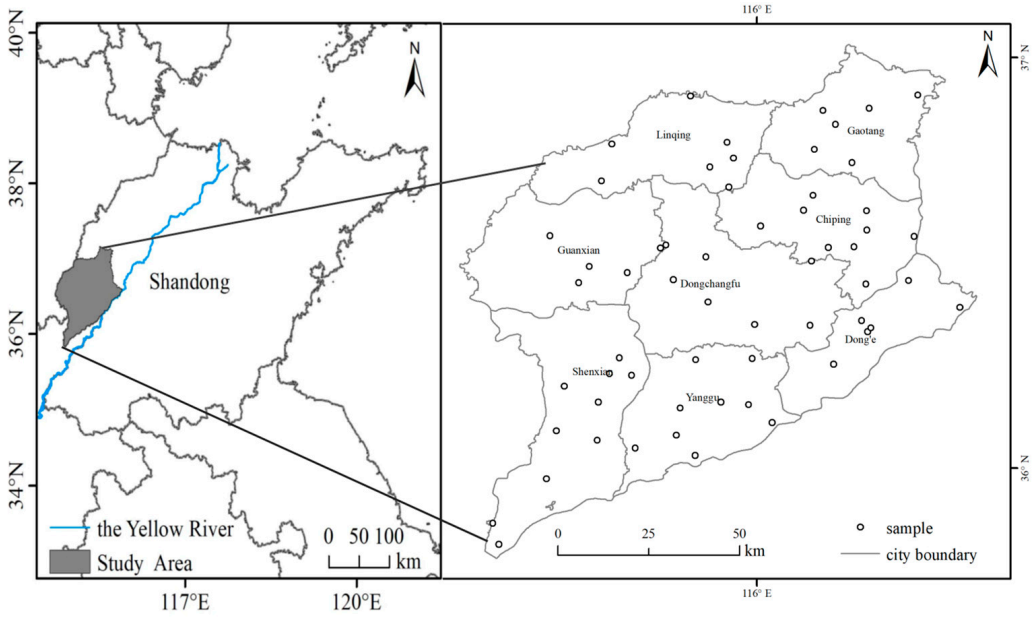


**Figure 1.** The study area location and sampling sites, circles refer to the sample site locations.

#### 2.1.2. Geology and Hydrogeology

The geomorphic type of the study region belonged to the Yellow River alluvial plain. Except for Paleozoic strata distributed in the southeast of the region, the rest are covered by Quaternary strata with a thickness ranging from 30 to 270 m. Generally, two types of aquifers can be classified within the Quaternary deposits: phreatic aquifer and confined aquifer, and the phreatic aquifer is the main aquifer for water supply [17], so this study mainly focused on it. The development, distribution and burial of the phreatic aquifer are affected by the Yellow River channel. In the main stream of the Yellow River channel, the phreatic aquifer is thicker. In the transition zone between the channel and the margin, the thickness of the phreatic aquifer is 5–15 m, with the lithology mainly composed of fine sand and silt. While in the marginal zone of the channel, the thickness of the aquifer is less than 5 m, with the lithology being silt and fine sand [18]. Groundwater replenishment in this area is mainly from precipitation and river and irrigation infiltration, and it is discharged through artificial extraction and evaporation.

### *2.2. Sample Collection and Analysis*

This study was a relatively long-term activity aimed to identify spatial–temporal changes in groundwater quality in Luxi Plain. Groundwater sample sites were evenly distributed throughout the study area, and samples were collected annually from 2018 to 2020. A total of 51, 60 and 60 samples from different sites were collected in August 2018, August 2019 and September 2020, respectively. The latitude/longitude of each sample site was accurately recorded with a portable GPS device.

At each sample site, the well was pumped for 15–20 min before sampling to ensure that the collected water could accurately reflect the status of local groundwater [19]. The parameters were analyzed using standard procedure. To measure pH and total dissolved solids (TDS), a portable pH/TDS meter (DZB-712F, Leici, Shanghai, China) was used during sampling. At the laboratory, calcium ($Ca^{2+}$), magnesium ($Mg^{2+}$), sodium ($Na^{+}$) and manganese ($Mn^{2+}$) were measured using a direct-reading inductively coupled plasma atomic emission spectrometer (ICAP6300, Thermo Scientific, Waltham, MA, USA). The detection limits of ICAP6300 for $Ca^{2+}$, $Mg^{2+}$, $Na^{+}$ and $Mn^{2+}$ were <0.002 mg/L, 0.02 mg/L, 0.02 mg/L and 0.05 mg/L, respectively. Ion chromatography (ICS-2100, Dionex, Sunnyvale, CA, USA) was adopted for analyzing chloride ($Cl^{-}$), sulfate ($SO_4{}^{2-}$), nitrate ($NO_3{}^{-}$), nitrite ($NO_2{}^{-}$) and fluoride ($F^{-}$) with the detection limits of <0.1 mg/L. Moreover, total hardness (TH), bicarbonate ($HCO_3{}^{-}$) and carbonate ($CO_3{}^{2-}$) were measured using titration

according to the standards described in Standard Methods for the Examination of Water and Wastewater, 20th edition [19]. The certified reference materials (provided by the China National Institute of Metrology, Beijing, China) were used to estimate analytical errors, which were usually below 5%.

For checking the anion–cation balance of each sample, ionic balance errors (E, %) were calculated, which can be expressed as follows [13].

$$E(\%) = \frac{\sum Ca - \sum An}{\sum Ca + \sum An} \times 100, \quad (1)$$

where Ca and An were the cations and anions in each sample, respectively. All the ions were expressed in milliequivalent per liter (meq/L) of each sample. It was commonly recognized that the ionic balance error (E) within ±10% was the acceptable data for study [20]. In this study, the E values of all samples were proved acceptable.

### *2.3. Entropy Water Quality Index*

EWQI was developed by integrating the concept of entropy weight into the traditional WQI [5]. In recent years, EWQI has gained widespread use in water quality evaluations because of its accuracy and reliability [5,21]. The detailed steps for calculating EWQI include the initial matrix $X_{ij}$ construction, data standardization, information entropy ($e_j$) calculation, entropy weight ($w_j$) and quality rating scale ($q_j$) calculation and EWQI calculation [4,5], as shown in Figure S1a. Due to the Chinese standard of pH ($S_{pH}$) ranges from 6.5 to 8.5, the pH quality rating scale ($q_{pH}$) needed to be calculated according to Equation(2) to ensure its value was positive [5].

$$q_{pH} = \frac{C_{pH} - 7}{S_{pH} - 7} \times 100, \quad (2)$$

where $C_{pH}$ was the detected pH value of each sample. $S_{pH}$ was determined by $C_{pH}$; if $C_{pH}$ was ≥7, $S_{pH}$ was 8.5, and while $C_{pH}$ was <7, $S_{pH}$ was 6. 5.

### *2.4. Human Health Risk Assessment*

In this study, the human health risk assessment (HHRA) model was adopted to describe the degree of potential risk to children and adults, which was established by the United States Environmental Protection Agency (USEPA) [22]. Generally, water environment pollution has a negative influence on human bodies via two main pathways: drinking (oral intake) and bathing (dermal intake) [23]. The potential risks reflected the additive effects of the two pathways. The detailed calculation processes and the parameters used for calculation can be found in the Supplementary Materials (Figure S1b and Table S2).

In this study, representative toxic indicators, such as manganese, fluoride, nitrate and nitrite, were selected as health evaluation parameters. The values of $RfD_{oral}$ (mg/(kg·d)), $RfD_{dermal}$ (mg/(kg·d)) and ABSgi (gastrointestinal absorption factor) for manganese were 0.14, 0.14 and 1, respectively [13,24,25]. For nitrate, the three values were 1.6, 1.6 and 1; for nitrite, they were 0.1, 0.1 and 1 and for fluoride, they were 0.04, 0.04 and 1, respectively [13,25]. If HI < 1, it indicated that the non-carcinogenic risk was acceptable; if HI > 1, it indicated that the risk was unacceptable and the groundwater will have an adverse effect on human health [24–26].

### *2.5. Statistical Analysis*

Groundwater quality and health risks analyses from 2018 to 2020 were performed via Kriging interpolation based on ArcGIS 10.7. The Piper and Gibbs analyses were implemented using Origin 2017.

## 3. Results and Discussion

### *3.1. Changes in Hydrochemical Characteristics of Groundwater*

To better understand the basic chemical characteristics of groundwater in Liaocheng, Luxi Plain, 11 physiochemical parameters were statistically analyzed. The detected values of these parameters and the drinking water quality limits for each parameter were listed in Table 1.

**Table 1.** Statistical summary of chemical compositions of groundwater in the study area.

| Parameters Chinese Standards [27]. | | pH - 6.5~8.5 | TDS mg/L 1000 | TH mg/L 450 | $Na^+$ mg/L 200 | Mn2+ mg/L 0.1 | $SO_4^{2-}$ mg/L 250 | $Cl^-$ mg/L 250 | $NO_3^-$ mg/L 20 | $F^-$ mg/L 1 | $NO2^-$ mg/L 1 | COD mg/L 3 |
|---|---|---|---|---|---|---|---|---|---|---|---|---|
| 2018 | Min | 6.91 | 613.0 | 323.0 | 33.5 | 0.01 | 29.1 | 43.6 | 0.40 | 0.31 | 0.003 | 0.05 |
| | Max | 7.76 | 7680.0 | 2450.0 | 1420.0 | 1.48 | 1790.0 | 1920.0 | 177.00 | 2.27 | 4.04 | 4.16 |
| | Mean | 7.39 | 2088.9 | 761.0 | 296.8 | 0.53 | 313.1 | 318.5 | 23.40 | 0.84 | 0.24 | 1.44 |
| | Std | 0.20 | 1058.7 | 391.4 | 254.7 | 0.33 | 331.3 | 348.5 | 39.30 | 0.45 | 0.79 | 0.87 |
| | CV (%) | 2.7 | 50.7 | 51.4 | 85.8 | 62.3 | 105.8 | 109.4 | 168.0 | 53.6 | 329.2 | 60.4 |
| 2019 | Min | 7.10 | 490.0 | 341.0 | 29.7 | 0.05 | 17.9 | 36.3 | 0.10 | 0.12 | 0 | 0.71 |
| | Max | 8.10 | 6184.0 | 2289.0 | 961.0 | 1.07 | 1795.0 | 1712.0 | 77.20 | 1.57 | 0.96 | 8.39 |
| | Mean | 7.46 | 1797.0 | 785.3 | 271.0 | 0.41 | 324.7 | 339.2 | 7.93 | 0.57 | 0.1 | 1.68 |
| | Std | 0.20 | 1186.5 | 364.4 | 205.7 | 0.28 | 326.6 | 339.7 | 17.10 | 0.36 | 0.25 | 1.41 |
| | CV (%) | 2.7 | 66.0 | 46.4 | 75.9 | 68.3 | 100.6 | 100.2 | 215.6 | 63.2 | 250.0 | 83.9 |
| 2020 | Min | 7.20 | 214.0 | 125.0 | 19.2 | 0.05 | 20.8 | 31.3 | 2.54 | 0.14 | 0 | 0.81 |
| | Max | 8.10 | 6836.0 | 2363.0 | 901.0 | 0.99 | 1921.0 | 1654.0 | 78.40 | 1.40 | 0.51 | 7.26 |
| | Mean | 7.60 | 1664.2 | 738.4 | 215.4 | 0.28 | 330.2 | 317.9 | 9.88 | 0.58 | 0.06 | 1.85 |
| | Std | 0.21 | 1209.1 | 368.4 | 178.2 | 0.27 | 340.4 | 331.7 | 12.36 | 0.31 | 0.15 | 1.05 |
| | CV (%) | 2.8 | 72.7 | 49.9 | 82.8 | 96.4 | 103.1 | 104.3 | 125.1 | 53.5 | 250.0 | 56.8 |

The pH is an important parameter that specifies whether the water is acidic or alkaline. The pH values varied from 6.91 to 7.76, 7.10 to 8.10 and 7.20 to 8.10, with average values of 7.39, 7.46 and 7.60 in 2018–2020, respectively. This indicated a slightly alkaline water quality in the study area. All the pH values were within the recommended range of 6.5 to 8.5 [27].

Total dissolved solids (TDS) represent the total amount of salt dissolved in the water [28]. In 2018–2020, TDS values showed a large range, from 214 to 7680 mg/L with the mean values of 2088.9, 1797.0 and 1664.2 mg/L, respectively. These values far exceeded the acceptable limits stipulated by China (<1000 mg/L), the World Health Organization [29] (<1000 mg/L) and the Central Pollution Control Board (<500 mg/L) [30]. Bai et al. [31] classified waters as freshwater (TDS < 1000 mg/L), brackish water (1000 $\leq$ TDS < 3000 mg/L) and saline water (3000 $\leq$ TDS < 10,000 mg/L) based on TDS content. Although the average TDS decreased during 2018–2020, 61.7% of the samples were still of the brackish water class and 6.7% of saline water in 2020. The high TDS levels in groundwater resulted from the high concentration of soluble fractions, such as $Na^+$, $Ca^{2+}$, $Mg^{2+}$, $Cl^-$ and $SO_4^{2-}$ (Table 1). Generally, TDS is used to reveal the degree of rock–water interactions, but irrigation return flows, domestic wastewater and chemical fertilizer infiltration can also affect TDS levels in groundwater [32,33].

The total hardness (TH) is principally caused by $Ca^{2+}$ and $Mg^{2+}$ in water [34,35]. The average values of TH in 2018–2020 were 761.0, 785.3 and 738.4 mg/L, respectively, exceeding the national standard stipulate of 450 mg/L [27]. Sawyer and McCarty [36] classified water based on its TH, which is soft when TH values were lower than 75 mg/L; moderately soft when values ranged from 76 to 150 mg/L; hard when values ranged between 151 and 300 mg/L and very hard when higher than 300 mg/L. Accordingly, the groundwater in this study region belonged to a very hard category. The changes in TH values during the three years were in line with that of the $Ca^{2+}$ and $Mg^{2+}$ concentrations.

$Na^+$ concentrations in the groundwater samples were in the range of 33.50–1420, 29.7–961 and 19.2–901 mg/L in 2018, 2019 and 2020, with averages of 296.8, 271.0 and 215.4 mg/L, respectively. Although the average values showed a decreasing trend from 2018 to 2020, more than 35% of samples failed to meet the relevant standard (<200 mg/L) in 2020. Among the trace metal cations, the superfluous manganese ($Mn^{2+}$) in the groundwater is relatively common, which can bring a series of adverse factors to daily life and industrial manufacturing. The concentration of $Mn^{2+}$ in more than 88% of samples exceeded the drinking standard (<0.1 mg/L) during 2018–2020, suggesting that $Mn^{2+}$ was an important indicator that affected the groundwater quality in this study area.

The changes in anion concentrations, such as $SO_4^{2-}$, $Cl^-$, $NO_3^-$, $F^-$ and $NO_2^-$ in groundwater, were also analyzed. The average concentrations of both $SO_4^{2-}$ and $Cl^-$ exceeded the maximum allowable limit in 2018–2020, and an increasing trend was observed, whereas $NO_3^-$, $F^-$ and $NO_2^-$ showed a subsequent decrease during these three years. Although the decreasing trend of the average value was observed, the highest $NO_3^-$ concentrations were still up to 77.20 and 78.40 mg-N/L in 2019 and 2020, respectively. The acceptable levels for drinking water quality, as defined by the WHO [29], China [37] and CPCB [30], are below 11.2 mg-N/L, 10 mg-N/L and 10 mg-N/L, respectively. The $NO_3^-$ concentration is primarily an indicator of anthropogenic activities. It was reported that the relationship of $NO_3^-/Na^+$ and $SO_4^{2-}/Na^+$ can reflect the impact of agricultural and industrial activities on groundwater [38]. In the present study region, the average values of $NO_3^-/Na^+$ were higher than 0.03 from 2018 to 2020, and the average values of $SO_4^{2-}/Na^+$ were lower than 1.53. These results indicated that the $NO_3^-$ in groundwater was mainly derived from agricultural activities. Indeed, higher agricultural practices have been observed in the study area, as agriculture is the primary economic source for the residents [39]. Most sample sites were located in agricultural areas, which resulted in a high $NO_3^-$ concentration in these samples, such as Houying, Zhouzhuang and Beijie sample sites located in Dongchangfu, Shenxian and Chiping, respectively. It was also found that the variation coefficients (CVs) of $NO_3^-$ and $NO_2^-$ were relatively high (Table 1), implying that they were the sensitive factors and their content varied with environmental changes.

Chemical oxygen demand (COD) concentration can reflect the extent of contamination in groundwater. The COD values of the samples ranged from 0.05 to 4.16 mg/L, 0.71 to 8.39 mg/L, 0.81 to 7.26 mg/L, with the mean of 1.44, 1.68 and 1.85 mg/L in 2018, 2019 and 2020, respectively. Most of the collected groundwater samples were within the allowable drinking water limit (<3.0 mg/L). Only three samples in 2018, two samples in 2019 and seven samples in 2020 were over the acceptable limit of drinking water.

Overall, TDS and TH in the study region were relatively high in 2018–2020, which exceeded the acceptable limit for drinking purposes. Although the concentration of major irons showed a decreasing trend from 2018 to 2020, the average concentrations of $Na^+$, $Mn^{2+}$, $SO_4^{2-}$ and $Cl^-$ still surpassed the drinking standard limit in 2020. COD and $NO_3^-$ are indicators of groundwater pollution, primarily caused by human activities [40]. The variation coefficients (CVs) of $NO_3^-$ and $NO_2^-$ were relatively high, indicating that the groundwater in the study region was polluted to varying degrees by agricultural activities. Additionally, the CVs of TDS, TH and other ions, except for $NO_3^-$ and $NO_2^-$, were low during the three years, suggesting that the contribution of water–rock interaction to water quality was larger than that of other factors in this region.

### *3.2. Sources of Ions and Controlling Factors*

The most reliable information on ion sources in groundwater can be predicted via Piper's trilinear diagram [41–43]. Figure 2 illustrated the hydrogeochemical characteristics of groundwater samples in 2018 and 2020. It can be seen that the Na + K facies type dominated in 2018, and there were almost no Ca type water, as shown in the lower left triangle of the Piper diagram. The sources of Na are complex, and the very high concentration of Na may be derived from a combination of rock mineral dissolution and human activities [44]. However, groundwater types continuously evolved to Ca types,

and the samples with Na + K facies type decreased from 56.9% to 16.7% in 2020. As indicated from the right triangle, the $HCO_3$ type predominated in both 2018 and 2020, at 74.5% in 2018 and 75.0% in 2020, followed by the no dominant type. Almost no $SO_4$ and Cl types of water were observed in the study area over the study period. It can be inferred that rock weathering plays a crucial role in determining the groundwater chemistry. Generally, different rock weathering results in varying combinations of ions in a solution [45]. For instance, Ca and Mg mainly originate from the weathering of carbonates, silicates and evaporites. Na and K originate from the weathering of evaporites and silicates. $HCO_3$ originates from carbonates and silicates, while $SO_4$ and Cl originate from evaporites [46]. In the study region, most of the ions are mainly derived from silicates and carbonates (Figure S2), which can be determined by the relationships of $[Mg^{2+}]/[Na^+]$ and $[Ca^{2+}]/[Na^+]$ [45]. Complex hydrogeochemical types of groundwater were observed from the upper diamond-shaped field. Nearly all samples belonged to $HCO_3$-Na, $HCO_3$-Ca·Mg and $SO_4$·Cl-Na types in 2018, whereas in 2020, a water type has evolved in which $HCO_3$-Na and $SO_4$·Cl-Na type water both decreased to 8.3%, and $SO_4$·Cl-Ca·Mg type water increased from 3.9% to 15%.

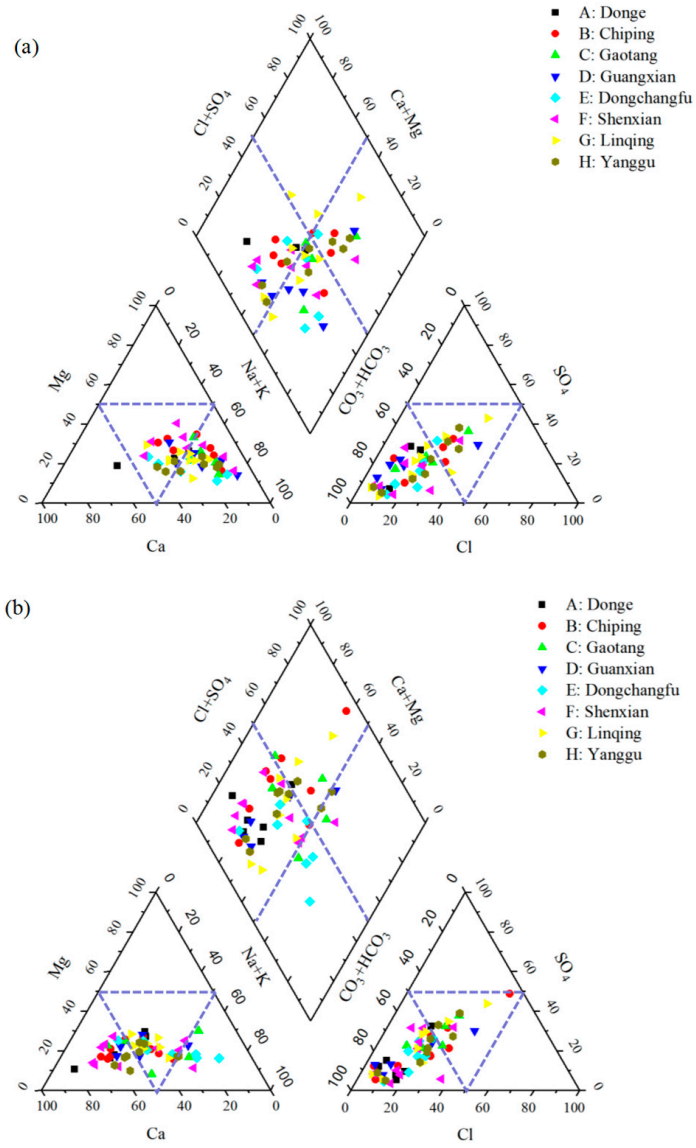


**Figure 2.** Piper diagram of groundwater samples in 2018 (**a**) and 2020 (**b**).

In conclusion, the chemical composition of groundwater was determined by rock weathering and also affected by anthropogenic activities during the study period. Cation exchange processes are non-obvious during the study period due to the poor relationship of [$Na^+$-$Cl^-$] and [$Ca^{2+}$+$Mg^{2+}$-$SO_4^{2-}$-$HCO_3^-$] ($R^2$ = 0.79 in 2018, 0.51 in 2020) [47], as shown in Figure S3. Moreover, there were differences in chemical types of groundwater in different counties, so groundwater in different counties should be used for different purposes.

Gibbs diagrams [48] can effectively illustrate the primary factors influencing the water quality. According to the diagram (Figure 3), a significant evolution of ions in the water was observed during 2018–2020. Almost all the samples were distributed in the rock dominance zone and evaporation dominance zone of the Gibbs plot, indicating that, apart from rock weathering processes, the groundwater hydrochemistry was also regulated by climatic factors. As groundwater flows underground and comes into active contact with rocks, water–rock interactions are generally the common factor that influences the evolution of natural groundwater chemistry [21]. Moreover, due to the fact that the study region is semi-arid, groundwater in this area experiences intense evaporation. Groundwater evaporation can elevate the concentrations of major ions and TDS, potentially leading to the precipitation of minerals, such as silicate and carbonate minerals. This phenomenon may cause the plots to shift towards the evaporation dominance zone on the Gibbs diagrams [21]. Notably, some samples were plotted out of the frame, and more samples were found in 2018. It was reported that the ion components of global water are almost always within the Gibbs plot, but when influenced by human activities, the samples may fall outside the frame [44]. This result was consistent with the ion source analysis mentioned above. Compared to 2020, groundwater in this region was more significantly affected by human activities in 2018.

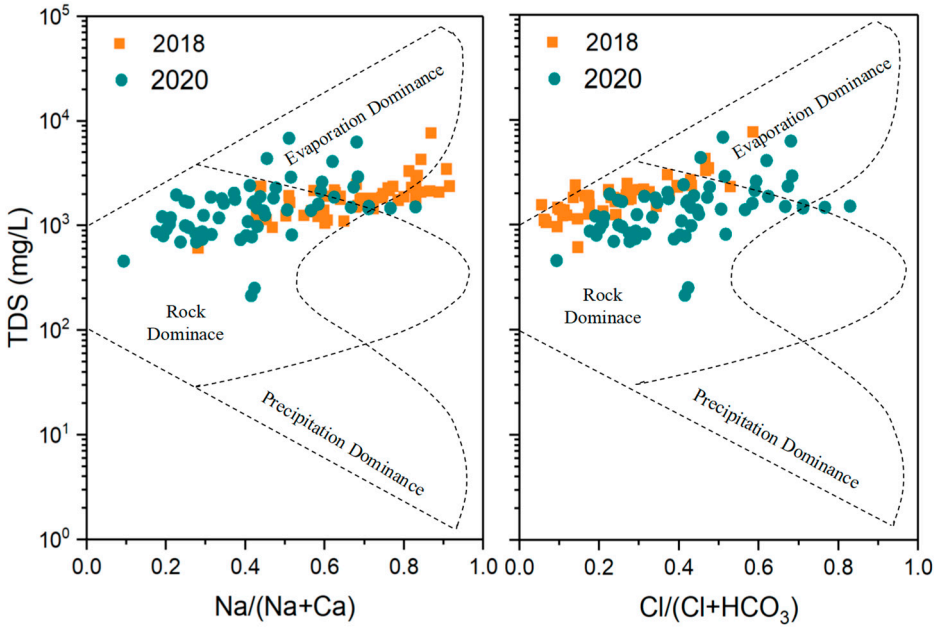


**Figure 3.** Gibbs diagrams of groundwater samples in 2018 and 2020.

### *3.3. Groundwater Quality Assessment*

In order to intuitively understand the groundwater quality in Luxi Plain, 11 parameters were selected to evaluate the water quality. The entropy weight ($W_j$) and entropy value ($W_j \times q_j$) of each parameter were calculated, as shown in Table 2. A high $W_j$ value indicated a large impact on groundwater quality [5]. During the study period, $NO_2^-$ has the highest $W_j$, followed by $NO_3^-$, revealing that nitrogenous materials have a larger influence on water quality than other parameters.

**Table 2.** Entropy weight and entropy value of each parameter.

| Items | Years | pH | TH | COD | $Cl^-$ | $SO4^{2-}$ | $Na^+$ | $NO3^-$ | $F^-$ | $Mn^{2+}$ | $NO2^-$ | TDS |
|---|---|---|---|---|---|---|---|---|---|---|---|---|
| Wj | 2018 | 0.02 | 0.05 | 0.03 | 0.10 | 0.09 | 0.06 | 0.21 | 0.06 | 0.03 | 0.32 | 0.04 |
| | 2019 | 0.02 | 0.04 | 0.11 | 0.07 | 0.07 | 0.05 | 0.26 | 0.08 | 0.04 | 0.21 | 0.05 |
| | 2020 | 0.03 | 0.03 | 0.08 | 0.10 | 0.10 | 0.07 | 0.15 | 0.05 | 0.08 | 0.26 | 0.05 |
| Wj × qj | 2018 | 0.44 | 8.28 | 1.47 | 12.15 | 11.05 | 9.02 | 48.18 | 4.90 | 17.95 | 7.71 | 8.38 |
| | 2019 | 0.73 | 7.21 | 6.26 | 9.81 | 8.93 | 6.47 | 20.96 | 4.26 | 14.81 | 2.12 | 8.92 |
| | 2020 | 1.16 | 5.04 | 4.94 | 12.32 | 12.58 | 7.52 | 13.93 | 3.10 | 14.52 | 1.70 | 8.78 |

In 2018, $NO_3^-$ had the highest entropy value, followed by $Mn^{2+}$, $Cl^-$ and $SO_4^{2-}$, while in 2019, the entropy value of all the parameters decreased, but $NO_3^-$ and $Mn^{2+}$ were still relatively high. In 2020, the entropy value of $Cl^-$ and $SO_4^{2-}$ were observed to elevate again. Various researchers have reported that nitrogenous substances are infrequent in the geological terrains, and the occurrence of nitrate in the groundwater was mainly of an anthropogenic nature [49,50]. While Mn is primarily derived from Mn-containing compounds in the primary sedimentary environment, the alkaline environment and high TDS in groundwater can promote the dissolution of Mn [51].

In the study area, the average EWQI value in 2018 was 129.5, indicating that the water quality was rated as class IV and, therefore, unsuitable for drinking. In 2019 and 2020, the values decreased to 90.5 and 94.0, and water quality was rated as class III (Table 3). In 2018, 19.6% of the samples were ranked as class II water quality, 45.10% were rated as class III and 9.8% and 25.5% were rated as class IV and V, respectively. In 2019 and 2020, the water quality remarkably changed for the better, the class V water decreased to 13.3% and 15.0%, respectively, indicating that the impact of human activities on groundwater quality decreased in 2019 and 2020. This result was in accordance with Section 3.2. Notably, the observed EWQI in 2020 was slightly higher than in 2019, which may mainly result from climatic factors. According to Table 3, 20.0% of the groundwater in the study area was of class I and II in 2020 and can be used directly for drinking. Additionally, 43.33% of class III groundwater could be used for domestic water; 36.67% of the groundwater belonged to class IV and V, which was completely non-potable for drinking purposes but can be used for irrigation and industrial production.

**Table 3.** Classification of groundwater quality based on EWQI.

| Value Range | Rank | 2018 (51) | Mean | 2019 (60) | Mean | 2020 (60) | Mean |
|---|---|---|---|---|---|---|---|
| EWQI < 25 | 1 | 0 | | 1 | | 3 | |
| 25 ≤ EWQI < 50 | 2 | 10 | | 18 | | 9 | |
| 50 ≤ EWQI < 100 | 3 | 23 | | 27 | 90.5 | 26 | 94.0 |
| 100 ≤ EWQI < 150 | 4 | 5 | 129.5 | 6 | | 13 | |
| 150 ≤ EWQI | 5 | 13 | | 8 | | 9 | |

EWQI spatial distribution maps were obtained with ArcGIS in 2018–2020 according to the EWQI rating system (Figure 4). The class III and IV groundwater zones almost covered the whole study area. From 2018 to 2020, the areas with class V groundwater zones decreased, while the areas with class III groundwater zones increased. The groundwater with class I and II quality was mainly distributed in the west of Guanxian and Linqing and southeast of Donge. The class V groundwater zones were mainly distributed in farmland areas of Guanxian, Linqing, Yanggu and Gaotang in 2020. Therefore, in the long run, the discharge of sewage and manure needs to be controlled. Moreover, precise and scientific fertilization based on local crop type needs to be studied in Liaocheng.

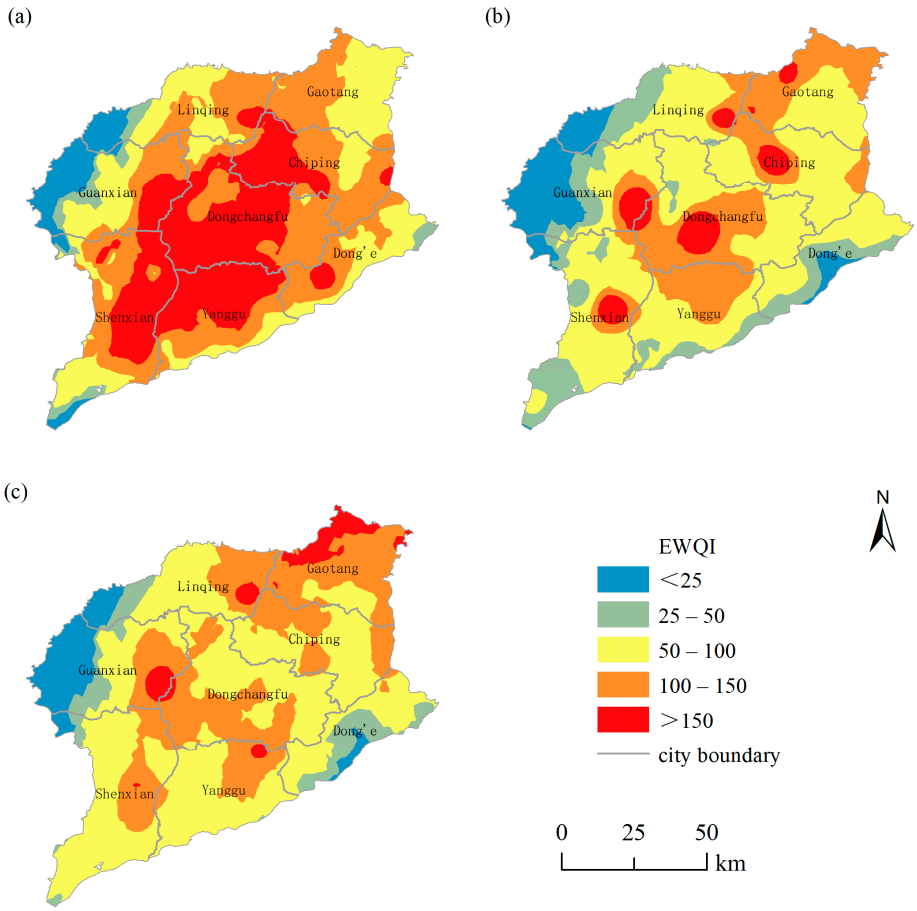


**Figure 4.** Spatial distribution maps of EWQI classification in 2018 (**a**), 2019 (**b**) and 2020 (**c**).

### *3.4. Health Risk Assessment*

As per EWQI, the groundwater in some sites was unsuitable for drinking. Consequently, the human health risk assessment in the study region is necessary, as some residents rely on groundwater for their drinking needs. As demonstrated in Table 4, the HI values varied from 0.35 to 3.65, with an average of 1.02 for adults in 2018, and from 0.64 to 6.84, with an average of 1.90 for children. In 2019, the HI values decreased, and the mean values were 0.50 for adults and 0.93 for children. However, the mean values of HI increased to 0.58 for adults and 1.08 for children in 2020. The potential risks were significantly higher in 2018 than in 2019 and 2020. Adults' health risk results revealed that 37.3%, 6.7% and 3.3% of the groundwater samples exceeded the non-carcinogenic risk limit of 1.0 in 2018–2020, while for children, they are 88.2%, 30.0% and 56.7%, respectively. Various studies have reported similar results that infants and children were at higher risk than adults [13]. The children were more susceptible to pollution because they consume more water and food in proportion to their body weight [4]. Moreover, the risk of non-carcinogenic effects through dermal contact was significantly lower compared to the risk associated with the ingestion pathway. The highest risks of dermal contact ($HQ_{dermal}$) for adults and children were 0.01 and 0.03 during the three years, respectively, while the highest risks caused by oral ingestion ($HQ_{oral}$) for adults and children are 3.65 and 6.81, respectively. This suggested that the risks from dermal contact can be considered negligible when compared to oral ingestion. Overall, the non-carcinogenic risk of groundwater in some sample sites was relatively high under assumed conditions, and there will certainly be impacts on more people's health if the groundwater in these sites was used for drinking in the future.

**Table 4.** Health risk results through different exposure pathways based on HHRA.

| Demographic | | | Min | Max | Mean | Median | Percentage of HI > 1 |
|---|---|---|---|---|---|---|---|
| 2018 | Adults | $HQ_{oral}$ | 0.34 | 3.65 | 1.01 | 0.75 | |
| | | $HQ_{dermal}$ | 0.00 | 0.01 | 0.00 | 0.00 | |
| | | HI | 0.35 | 3.65 | 1.02 | 0.75 | 19 (37.3%) |
| | Children | $HQ_{oral}$ | 0.64 | 6.81 | 1.89 | 1.40 | |
| | | $HQ_{dermal}$ | 0.00 | 0.03 | 0.01 | 0.01 | |
| | | HI | 0.64 | 6.84 | 1.90 | 1.40 | 45 (88.2%) |
| 2019 | Adults | $HQ_{oral}$ | 0.12 | 1.93 | 0.49 | 0.44 | |
| | | $HQ_{dermal}$ | 0.00 | 0.01 | 0.00 | 0.00 | |
| | | HI | 0.12 | 1.94 | 0.50 | 0.44 | 4 (6.7%) |
| | Children | $HQ_{oral}$ | 0.22 | 3.60 | 0.92 | 0.82 | |
| | | $HQ_{dermal}$ | 0.00 | 0.01 | 0.00 | 0.00 | |
| | | HI | 0.23 | 3.61 | 0.93 | 0.83 | 18 (30.0%) |
| 2020 | Adults | $HQ_{oral}$ | 0.18 | 1.66 | 0.58 | 0.55 | |
| | | $HQ_{dermal}$ | 0.00 | 0.01 | 0.00 | 0.00 | |
| | | HI | 0.18 | 1.66 | 0.58 | 0.55 | 2 (3.3%) |
| | Children | $HQ_{oral}$ | 0.34 | 3.09 | 1.08 | 1.02 | |
| | | $HQ_{dermal}$ | 0.00 | 0.01 | 0.00 | 0.00 | |
| | | HI | 0.34 | 3.10 | 1.08 | 1.02 | 34 (56.7%) |

Table 5 presented the statistical summary of HQ values for manganese, fluoride, nitrate and nitrite in groundwater samples during the three years. The contributions of non-carcinogenic risk to adults and children in 2018–2020 were as follows: fluoride > nitrate > manganese > nitrite. Fluoride is widely distributed in the Earth's crust and can be found in several fluoride-rich minerals, including ($CaF_2$), fluorapatite ($Ca_5(PO_4)_3F$), villiaumite (NaF) and topaz ($Al_2(SiO_4)F_2$) [52,53]. High $HCO_3^-$ and $Na^+$ and low $Ca^{2+}$ can enrich the $F^-$ in groundwater [53]. Furthermore, the groundwater in the study area exhibited an alkaline condition, which is conducive to the dissolution of fluoride minerals [23,54].

**Table 5.** Statistical summary of HQ and HI values for adults and children.

| Demographic | | | $Mn^{2+}$ | $F^-$ | $NO_3^-$ | $NO_2^-$ | HI |
|---|---|---|---|---|---|---|---|
| 2018 | Adults | Min | 0.00 | 0.19 | 0.01 | 0.00 | 0.34 |
| | | Max | 0.26 | 1.43 | 2.77 | 1.01 | 3.65 |
| | | Mean | 0.09 | 0.53 | 0.34 | 0.06 | 1.02 |
| | Children | Min | 0.00 | 0.36 | 0.01 | 0.00 | 0.64 |
| | | Max | 0.50 | 2.66 | 5.18 | 1.89 | 6.84 |
| | | Mean | 0.17 | 0.98 | 0.63 | 0.11 | 1.90 |
| 2019 | Adults | Min | 0.01 | 0.06 | 0.00 | 0.00 | 0.12 |
| | | Max | 0.19 | 0.99 | 1.21 | 0.24 | 1.94 |
| | | Mean | 0.07 | 0.31 | 0.09 | 0.03 | 0.50 |
| | Children | Min | 0.02 | 0.12 | 0.00 | 0.00 | 0.23 |
| | | Max | 0.36 | 1.84 | 2.26 | 0.45 | 3.61 |
| | | Mean | 0.13 | 0.58 | 0.16 | 0.05 | 0.93 |
| 2020 | Adults | Min | 0.01 | 0.00 | 0.04 | 0.00 | 0.18 |
| | | Max | 0.18 | 0.88 | 1.23 | 0.13 | 1.66 |
| | | Mean | 0.05 | 0.36 | 0.16 | 0.02 | 0.58 |
| | Children | Min | 0.02 | 0.00 | 0.07 | 0.00 | 0.34 |
| | | Max | 0.33 | 1.64 | 2.30 | 0.24 | 3.10 |
| | | Mean | 0.09 | 0.67 | 0.29 | 0.03 | 1.08 |

In addition, the spatial distribution results of non-carcinogenic health risks for children and adults in 2018–2020 were shown in Figure 5. The health risks for adults and children

decreased from 2018 to 2020. The total non-carcinogenic risks virtually all occur in Shenxian, Yanggu and Dongchangfu in 2019 and 2020. Shenxian is the largest agricultural county in Liaocheng, followed by Yanggu [39], implying that the fertilizer may be the biggest threat to human health in these two areas. Dongchangfu has the largest economic output value in Liaocheng [39], so the high risk in this region should be attributed to human activities and special geological conditions. Consequently, treatment and remediation for groundwater with high levels of fluoride, manganese and nitrate need to be carried out in these regions. Moreover, policies should be developed to prevent and control pollution sources.

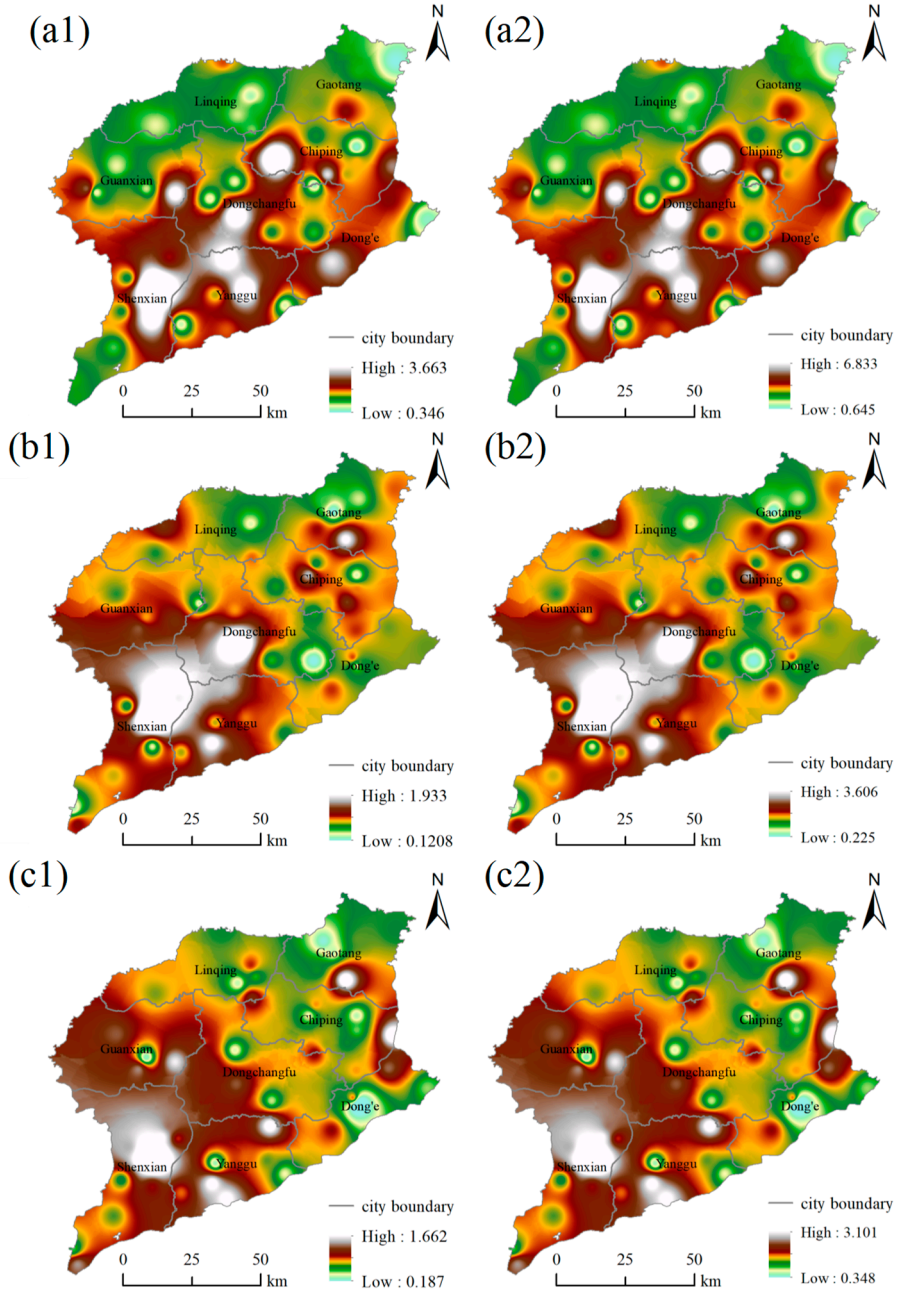


**Figure 5.** Spatial distribution maps of health risks in 2018 (**a**), 2019 (**b**) and 2020 (**c**): adults (**1**), children (**2**).

## 4. Conclusions

Groundwater plays a crucial role in the natural water cycle and is a vital source of the global water supply. The results observed that the hydrochemical characteristics of

groundwater in the study area evolved from 2018 to 2020 due to water–rock interactions, climatic factors and human activities. The ions in groundwater were mainly derived from silicate and carbonate weathering, and the cation exchange processes were not obvious. Moreover, the groundwater quality was found to get better over time based on the EWQI; 31.67% of the groundwater samples in 2019 and 20.00% in 2020 in the study area were of class I and II quality and can be used directly for drinking, while others can be used for domestic water or irrigation. The groundwater with class I and II quality was distributed in the west and southeast of the study area. Furthermore, the results of the HHRA showed that the non-carcinogenic risk contributions to adults and children in 2018–2020 were in the order of fluoride > nitrate > manganese > nitrite. The spatial distribution maps indicated that the high health risks in 2019 and 2020 virtually all occurred in the counties or districts with higher agricultural or economic values. The outcomes of this study are expected to assist governing bodies in developing effective strategies for improving drinking water management.

**Supplementary Materials:** The following supporting information can be downloaded at: https://www.mdpi.com/article/10.3390/w15234120/s1, Table S1: Statistical summary of water chemical compositions in other area of the world; Table S2: Key parameters used in the human health risk assessment; Figure S1: The processes of calculating EWQI (a) and human health risk assessment (b); Figure S2: The relationship of Mg/Na and Ca/Na in groundwater of Liaocheng in 2018 and 2020; Figure S3: The relationship of $Na^+$-$Cl^-$ and $Ca^{2+}$+$Mg^{2+}$-$SO_4{}^{2-}$-$HCO_3{}^-$ in groundwater of Liaocheng in 2018 (a) and 2020 (b).

**Author Contributions:** Conceptualization, Y.L.; Investigation, N.Y. and G.L.; Methodology, N.Y.; Supervision, Y.L., G.L., F.Z. and Q.W.; Visualization, N.Y. and Q.W.; Writing–original draft, N.Y. and Y.L.; Writing–review and editing, Y.L., G.L., F.Z. and Q.W. All authors have read and agreed to the published version of the manuscript.

**Funding:** This research was funded by the Doctoral Foundation of Liaocheng University (318051904), and the Natural Science Foundation of Shandong Province (ZR2022MD063).

**Data Availability Statement:** The data that support the findings of this study are available from the corresponding author upon reasonable request.

**Conflicts of Interest:** The authors declare that they have no conflict of interest.

## References

1. Li, P.; He, X.; Li, Y.; Xiang, G. Occurrence and health implication of fluoride in groundwater of loess aquifer in the Chinese Loess Plateau: A case study of Tongchuan, northwest China. *Expo. Health* **2019**, *11*, 95–107. [CrossRef]
2. Mthembu, P.P.; Elumalai, V.; Senthilkumar, M.; Wu, J. Investigation of geochemical characterization and groundwater quality with special emphasis on health risk assessment in alluvial aquifers, South Africa. *Int. J. Environ. Sci. Technol.* **2021**, *18*, 3711–3730. [CrossRef]
3. He, X.; Wu, J.; Guo, W. Karst spring protection for the sustainable and healthy living: The examples of Niangziguan spring and Shuishentang spring in Shanxi, China. *Expo. Health* **2019**, *11*, 153–165. [CrossRef]
4. Wang, Y.; Li, P. Appraisal of shallow groundwater quality with human health risk assessment in different seasons in rural areas of the Guanzhong Plain (China). *Environ. Res.* **2022**, *207*, 112210. [CrossRef]
5. Wang, D.; Wu, J.; Wang, Y.; Ji, Y. Finding high-quality groundwater resources to reduce the hydatidosis incidence in the Shiqu County of Sichuan Province, China: Analysis, assessment, and management. *Expo. Health* **2020**, *12*, 307–322. [CrossRef]
6. Su, F.; Wu, J.; He, S. Set pair analysis-Markov chain model for groundwater quality assessment and prediction: A case study of Xi'an city, China. *Hum. Ecol. Risk Assess.* **2019**, *12*, 343–354. [CrossRef]
7. Farzaneh, G.; Khorasani, N.; Ghodousi, J.; Panahi, M. Assessment of surface and groundwater resources quality close to municipal solid waste landfill using multiple indicators and multivariate statistical methods. *Int. J. Environ. Res.* **2021**, *15*, 383–394. [CrossRef]
8. Ustaoğlu, F.; Tepe, Y.; Taş, B. Assessment of stream quality and health risk in a subtropical Turkey river system: A combined approach using statistical analysis and water quality index. *Ecol. Indic.* **2019**, *113*, 105815. [CrossRef]
9. Elham, F.; Sahar, M. Assessment of hydrochemical characteristics and groundwater suitability for drinking and irrigation purposes in Garmsar Plain, Iran. *Geopersia* **2023**, *13*, 83–102.
10. Mansi, T.; Sunil, K.S. Allocation of weights using factor analysis for development of a novel water quality index. *Ecotoxicol. Environ. Saf.* **2019**, *183*, 109510.

11. Singh, G.; Rishi, M.S.; Herojeet, R.; Kaur, L.; Sharma, K. Evaluation of groundwater quality and human health risks from fluoride and nitrate in semi-arid region of northern India. *Environ. Geochem. Health* **2020**, *42*, 1833–1862. [CrossRef] [PubMed]
12. Ji, Y.; Wu, J.; Wang, Y.; Elumalai, V.; Subramani, T. Seasonal variation of drinking water quality and human health risk assessment in Hancheng City of Guanzhong Plain, China. *Expo. Health* **2020**, *12*, 469–485. [CrossRef]
13. Adimalla, N.; Qian, H. Groundwater quality evaluation using water quality index (WQI) for drinking purposes and human health risk (HHR) assessment in an agricultural region of Nanganur, south India. *Ecotoxicol. Environ. Saf.* **2019**, *176*, 153–161. [CrossRef] [PubMed]
14. Karunanidhi, D.; Subramani, T.; Deepali, M.; Aravinthasamy, P.; Bellows, B.C.; Li, P. Groundwater quality evolution based on geochemical modeling and aptness testing for ingestion using entropy water quality and total hazard indexes in an urban-industrial area (Tiruppur) of southern India. *Environ. Sci. Pollut. Res.* **2021**, *28*, 18523–18538. [CrossRef] [PubMed]
15. Liaocheng Water Resources Bureau. *Water Resources Bulletin of Liaocheng*; Liaocheng Water Resources Bureau: Liaocheng, China, 2021. (In Chinese)
16. Li, Y.; Liu, S.M.; Yu, J.; Hu, Z.F.; Shao, L.J. Study on water quality characteristics and causes of shallow groundwater in suburbs of Liaocheng City. *Environ. Sci. Manag.* **2020**, *6*, 57–62. (In Chinese)
17. Wu, J.; Sun, Z. Evaluation of shallow groundwater contamination and associated human health risk in an alluvial plain impacted by agricultural and industrial activities, mid-west China. *Expo. Health* **2016**, *8*, 311–329. [CrossRef]
18. Yu, H.C.; Liu, X.Z.; Zhang, G.Y. Exploration and management of shallow groundwater over-exploitation area in Luxi Plain. *Groundwater* **2010**, *4*, 24–25. (In Chinese)
19. APHA. *Standard Methods for the Examination of Water and Wastewater*, 20th ed.; American Public Health Association: Washington, DC, USA, 1999.
20. Domenico, P.A.; Schwartz, F.W. *Physical and Chemical Hydrogeology*; Wiley: New York, NY, USA, 1990.
21. Li, P.; He, X.; Guo, W. Spatial groundwater quality and potential health risks due to nitrate ingestion through drinking water: A case study in Yan'an City on the Loess Plateau of northwest China. *Hum. Ecol. Risk Assess.* **2019**, *25*, 11–31. [CrossRef]
22. Adimalla, N.; Sanda, R. Spatial distribution and seasonal variation in fluoride enrichment in groundwater and its associated human health risk assessment in Telangana State, South India. *Hum. Ecol. Risk Assess.* **2018**, *24*, 2119–2132.
23. Chen, J.; Wu, H.; Qian, H. Groundwater nitrate contamination and associated health risk for the rural communities in an agricultural area of Ningxia, northwest China. *Expo. Health* **2016**, *8*, 349–359. [CrossRef]
24. USEPA, (US Environmental Protection Agency). *Baseline Human Health Risk Assessment*; Vasquez Boulevard and I-70 Superfund Site; USEPA: Denver, CO, USA, 2001.
25. USEPA. *Risk Assessment Guidance for Superfund Volume I: Human Health Evaluation Manual (Part E)*; USEPA: Denver, CO, USA, 2004.
26. Adimalla, N.; Li, P. Occurrence, health risks, and geochemical mechanisms of fluoride and nitrate in groundwater of the rock-dominant semi-arid region, Telangana State, India. *Hum. Ecol. Risk Assess. Int. J.* **2018**, *25*, 81–103. [CrossRef]
27. *GB/T 14848–2017*; Standard for Groundwater Quality. Inspection and Quarantine of the P.R. China. China Standard Press: Beijing, China, 2017. (In Chinese)
28. Subba Rao, N.; Marghade, D.; Dinakar, A.; Chandana, I.; Sunitha, B.; Ravindra, B.; Balaji, T. Geochemical characteristics and controlling factors of chemical composition of groundwater in a part of Guntur district, Andhra Pradesh, India. *Environ. Earth Sci.* **2017**, *76*, 747. [CrossRef]
29. WHO (World Health Organisation). *Guidelines for Drinking Water Quality*; WHO: Geneva, Switzerland, 2011; Volume 92, pp. 15–18.
30. CPCB (Central Pollution Control Board). *Guidelines for Drinking Water Quality in India*; CPCB: Delhi, India, 2018.
31. Bai, F.; Zhou, J.; Zeng, Y. Hydrochemical characteristics and quality of groundwater in the plains of the Turpan Basin. *Arid Zone Res.* **2022**, *39*, 419–428. (In Chinese)
32. Duraisamy, S.; Govindhaswamy, V.; Duraisamy, K.; Krishinargaj, S.; Balasubramanian, A.; Thirumalaisamy, S. Hydrogeochemical characterization and evaluation of groundwater quality in Kangayam taluk, Tirupur district, Tamil Nadu, India, using GIS techniques. *Environ. Geochem. Health* **2019**, *41*, 851–873. [CrossRef]
33. Karakus, C.B. Evaluation of groundwater quality in Sivas province (Turkey) using water quality index and GIS-based analytic hierarchy process. *Int. J. Environ. Health Res.* **2019**, *29*, 500–519. [CrossRef]
34. Li, P.; Wu, J.; Qian, H.; Lyu, X.; Liu, H. Origin and assessment of groundwater pollution and associated health risk: A case study in an industrial park, northwest China. *Environ. Geochem. Health* **2014**, *36*, 693–712. [CrossRef]
35. Liu, Y.; Luo, K.; Lin, X.; Gao, X.; Ni, R.; Wang, S.; Tian, X. Regional distribution of longevity population and chemical characteristics of natural water in Xinjiang, China. *Sci. Total Environ.* **2014**, *473–474*, 54–62. [CrossRef]
36. Sawyer, C.N.; McCarty, P.L. *Chemistry for Sanitary Engineers*, 2nd ed.; McGraw Hill: New York, NY, USA, 1967.
37. *GB5749–2022*; Standard for Groundwater Quality. State Administration for Market Regulation, Standardization Administration. China Standard Press: Beijing, China, 2022. (In Chinese)
38. Zhang, Q.; Qian, H.; Xu, P.; Liu, R. Effect of hydrogeological conditions on groundwater nitrate pollution and human health risk assessment of nitrate in Jiaokou irrigation district. *J. Clean. Prod.* **2021**, *298*, 126783. [CrossRef]
39. Liaocheng Statistic Bureau. *Liaocheng Statistical Yearbook*; China Statistics Press: Beijing, China, 2022. (In Chinese)
40. Peng, C.; He, J.T.; Wang, M.L.; Zhang, Z.G.; Wang, L. Identifying and assessing human activity impacts on groundwater quality through hydrogeochemical anomalies and $NO_3^-$, $NH_4^+$, and COD contamination: A case study of the Liujiang River Basin, Hebei Province, P.R. China. *Environ. Sci. Pollut. Res.* **2018**, *25*, 3539–3556. [CrossRef]

41. Piper, A. A graphic procedure in the geochemical interpretation of water-analysis. *Trans. Am. Geophys. Union* **1944**, *25*, 914–928.
42. He, S.; Li, P. A MATLAB based graphical user interface (GUI) for quickly producing widely used hydrogeochemical diagrams. *Geochemistry* **2020**, *80*, 125550. [CrossRef]
43. Su, Z.; Wu, J.; He, X.; Elumalai, V. Temporal changes of groundwater quality within the groundwater depression cone and prediction of confined groundwater salinity using grey Markov model in Yinchuan area of northwest China. *Expo. Health* **2020**, *12*, 447–468. [CrossRef]
44. Tu, C.; Yang, R.; Ma, Y.; Linghu, C.; Zhao, R.; He, C. Characteristics and driving factors of hydrochemical evolution in Tuochangjiang River Basin, western Guizhou Province. *Environ. Sci.* **2023**, *44*, 740–751. (In Chinese)
45. Jiang, L.; Yao, Z.; Liu, Z.; Wang, R.; Wu, S. Hydrochemistry and its controlling factors of rivers in the source region of the Yangtze River on the Tibetan Plateau. *J. Geochem. Explor.* **2015**, *155*, 76–83. [CrossRef]
46. Chen, J.; Wang, F.; Xia, X.; Zhang, L. Major element chemistry of the Changjiang (Yangtze River). *Chem. Geol.* **2002**, *187*, 231–255. [CrossRef]
47. Wang, H.; Jiang, X.; Wan, L. Hydrogeochemical characterization of groundwater flow systems in the discharge area of a river basin. *J. Hydrol.* **2015**, *527*, 433–441. [CrossRef]
48. Gibbs, R.J. Mechanisms controlling world water chemistry. *Science* **1970**, *170*, 795–840. [CrossRef] [PubMed]
49. Maila, Y.A.; EI-Nahal, I.; Al-Agha, M.R. Seasonal variations and mechanisms of groundwater nitrate pollution in the Gaza Strip. *Environ. Geol.* **2004**, *47*, 84–90. [CrossRef]
50. Biddau, R.; Dore, E.; Da Pelo, S.; Lorrai, M.; Botti, P.; Testa, M.; Cidu, R. Geochemistry, stable isotopes and statistic tools to estimate threshold and source of nitrate in groundwater (Sardinia, Italy). *Water Res.* **2023**, *232*, 119663. [CrossRef]
51. Lv, X.; Liu, J.; Zhu, L.; Liu, J.; Liu, C. Distribution and source of Fe and Mn in groundwater of Lanzhou City. *J. Arid Land Res. Environ.* **2019**, *33*, 130–136. (In Chinese)
52. Adimalla, N.; Li, P.; Qian, H. Evaluation of groundwater contamination for fluoride and nitrate in semi-arid region of Nirmal Province, South India: A special emphasis on human health risk assessment (HHRA). *Hum. Ecol. Risk Assess.* **2019**, *25*, 1107–1124. [CrossRef]
53. Adimalla, N.; Wu, J. Groundwater quality and associated health risks in a semiarid region of south India: Implication to sustainable groundwater management. *Hum. Ecol. Risk Assess.* **2019**, *25*, 191–216. [CrossRef]
54. Jalali, M. Nitrate pollution of groundwater in Toyserkan, western Iran. *Environ. Earth Sci.* **2011**, *62*, 907–913. [CrossRef]